COMPARISON BETWEEN THE CCD CZT AND THE DIGITAL FFT

D. D. Buss, R. L. Veenkant, R. W. Brodersen, and C. R. Hewes

Texas Instruments Incorporated
Dallas, Texas 75222

Sponsored by:
ECOM / Bob Sprout
NOSC / Whitehurst
NRRA / Bond.

ABSTRACT. The CCD analog transversal filter is a tremendously cost-effective component in terms of its simplicity compared to equivalent digital hardware. In view of this, the chirp z-transform (CZT) algorithm for performing spectral analysis is ideally suited to CCD implementation because, in this algorithm, the bulk of the computation is performed in a transversal filter. The CCD CZT has some performance limitations relative to the digital fast Fourier transform (FFT), and for this reason, it is not applicable to all military signal processing systems. However, for those applications which fall within the CCD performance capabilities, the CZT offers significant potential cost saving over the digital FFT. The performance of the CCD CZT is evaluated and compared with the digital FFT. A discussion is given of selected military applications where the CCD CZT can be used to advantage.

I. INTRODUCTION

Charge-coupled device (CCD) analog transversal filters can be used to perform the discrete Fourier transform (DFT) on electrical signals using an algorithm called the chirp z-transform (CZT).[1,2] The CCD CZT has been demonstrated,[3,4] and it has been proposed as a replacement for the digital fast fourier transform (FFT), in a number of military signal processing applications.[5] It is the purpose of this paper to compare the CCD CZT with the digital FFT.

In a general way, the comparison can be summarized as follows. The CCD CZT has performance limitations when compared with the digital FFT, and it is somewhat less flexible. However, it has a tremendous projected cost advantage when manufactured in high volume, and has additional advantages in smaller size, lighter weight, lower power and improved reliability. Although the CCD CZT has modest performance, significant cost advantages can be realized for those applications which fall within its performance capabilities. It is the goal of this paper to quantitatively compare the CCD CZT with the digital FFT and to identify a few major military applications in which the CCD CZT is certain to be important.

Section II reviews conventional digital spectrum analysis techniques; the digital FFT and the deltec spectrum analyzer. Section III discusses the CCD CZT and a related prime transform. Section IV compares the CCD CZT with the digital FFT in error, resolution and implementation, and Section V discusses selected military applications of modest required performance for which the CCD CZT has clear cost advantages over digital implementation.

II. REVIEW OF DIGITAL SPECTRAL ANALYSIS METHODS

The FFT is currently the most widely used technique for digital spectral analysis. It is important because it requires only $N/2 \log_2 N$ complex multiply operations to perform an N-point DFT, as compared with N^2 complex multiply operations required to directly implement the DFT formula

$$F_k = \sum_{n=0}^{N-1} f_n e^{-i2\pi nk/N} \qquad (1)$$

The deltec spectrum analyzer historically preceeded the FFT, and has been largely replaced except in certain sonar spectrum analysis applications.

FFT

The FFT algorithm is discussed from an elementary point of view in References 6, 7 and 8. In this section, it will be reviewed for the purposes of establishing nomenclature for discussion in later sections.

FFT algorithms can be classed as decimation in time or decimation in frequency. The former is discussed here, but the latter is quite similar. The most common FFT algorithms are radix 2, meaning that the entire FFT is performed by sequential operations involving only pairs of elements. The fundamental operation in a radix 2 FFT is the so-called butterfly which takes two complex inputs A and B and combines them to give X and Y through the operation

$$X = A + W_N^k B$$
$$Y = A - W_N^k B \qquad (2)$$

where $W_N \equiv \exp[-i2\pi/N]$, and the W_N^k are the so-called twiddle factors. The butterfly structure is indicated schematically in Figure 1a, using the the notation of Reference 8.

An 8-point, radix 2, decimation-in-time, FFT algorithm is illustrated in Figure 1b. The data are first reordered by bit reversal,[8] and the first set of butterflies essentially performs the 2-point DFT on the reordered input data by pairs. The second set of butterflies combines the 2-point DFT's using twiddle factors to achieve two 4-point DFT's on the even and odd numbered input data. The final set of butterflies combines the 4-point DFT's using twiddle factors to achieve the final 8-point DFT.

Several important facts about radix 2 FFT's are apparent from the above discussion: (1) N must be an integral power of two. (2) There are $\log_2 N$ stages each requiring N/2 butterfly operations for a total of N/2 $\log_2 N$ butterflies required, and (3) Each Fourier coefficient is processed through $\log_2 N$ butterfly operations so that quantization errors are cumulative.

In many applications, the FFT is used to obtain a transform which will later be inverted to obtain the original signal. In such applications, the phase of the transform must be maintained. However, in many other cases it is desired to obtain a measure of the spectral energy density of a quasi-periodic waveform or a quasi- stationary random process. For these applications, the phase of the transform is not important. In addition, the true DFT is not performed, but the input data are apodized or windowed by an appropriate windowing function w_n to suppress frequency sidelobes in the spectrum.[6,7,8] The desired result is

$$|F_k|^2 = \left| \sum_{n=0}^{N-1} f_n w_n e^{-i2\pi nk/N} \right|^2 \qquad (3)$$

For even moderate values of N the computational saving of the FFT algorithm is extremely significant, and for common spectrum analysis applications the savings is easily a factor of 10 to 100. The FFT is flexible enough and powerful enough to be considered a general purpose spectrum analysis tool.

DELTIC SPECTRUM ANALYZER

The deltic spectrum analyzer has been implemented in analog, digital and hybrid technologies. It is essentially a straightforward implementation of equation (1) in which the time series f_n is stored in a circulating delay line, usually in digital form. A complete circulation of the time sequence is performed in the time between each newly acquired input sample. During this circulation, the f_n are operated on either digitally or analog to form a spectral estimate at a selected frequency. To obtain a complete spectrum at N frequencies requires N^2 operations. However, N is not restricted to be a power of 2, and the frequencies are not restricted to be of uniform spacing as in the DFT. Often, one-bit quantization is used to represent the f_n. This minimizes hardware requirements but results in significant detection loss and small signal suppression effects.[9]

III. CCD SPECTRAL ANALYSIS TECHNIQUES

From the standpoint of minimizing the number of digital operations required to perfprm the DFT, the FFT algorithm is optimal. However, in determining the optimum algorithm for implementation with analog CCD's, a whole new set of ground rules exists. It is no longer important to minimize multiplications, because CCD transversal filters can be built which perform a large number of multiplications simultaneously in real time time.[10,11,12,13,14,15] Consequently, for

CCD implementation, algorithms should be selected in which the bulk of the computation is performed by a transversal filter. Two such algorithms have been identified for cost-effective CCD implementation; the CZT[1,2] and the prime transform.[16,17] Both algorithms are discussed in this section.

CCD CZT

The DFT can be performed using the chirp z-transform (CZT) algorithm.[2] The CZT gets its name from the fact that it can be implemented by (1) premultiplying the time signal with a chirp (linear FM) waveform, (2) filtering in a chirp convolution filter, and (3) postmultiplying with a chirp waveform. When implemented digitally, the CZT has no clear cut advantages over the conventional FFT algorithm.[2] However, the CZT lends itself naturally to implementation with CCD transversal filters.[1]

Starting with the definition of the DFT given in equation (1), and using the substitution

$$2nk = n^2 + k^2 - (n - k)^2 \tag{4}$$

the following equation results:

$$F_k = e^{-i\pi k^2/N} \cdot \sum_{n=0}^{N-1} \left(f_n e^{-i\pi n^2/N} \right) e^{i\pi (k - n)^2/N} \tag{5}$$

This equation has been factored to emphasize the three operations which make up the CZT algorithm. It is illustrated in Figure 2.

To implement the conventional N-point CZT, the CCD filters are chirp filters of length 2N-1 which chirp from $-f_c$ to $+f_c$, and the premultiply waveform has a time duration N/f_c and chirps from zero to $-f_c$. A physical interpretation in terms of correlation of the input chirp with the filter is given in Figure 3. When the input signal has zero frequency, the product with the premultiply chirp results in an input waveform to the filter which chirps from 0 to $-f_c$. The samples corresponding to frequencies near f = 0 are clocked into the filter first, and those near $f = -f_c$ are clocked in last. This sequence of samples results in a correlation peak at $t = t_o$, when the product waveform has been clocked into the first half of the filter. When the input frequency is $f_1 \neq 0$, the product with the premultiply chirp results in an input to the filter which chirps from f_1 to $-f_c + f_1$. The input waveform (V_{in} x chirp) in Figure 3 corresponds to an input signal at a frequency f_1 at time $t = t_o$. This waveform is shifted to the right as t increases resulting in a correlation peak at t_1. The shift in time relative to the dc correlation peak is

$$t_1 - t_o = \frac{N}{f_c^2} f_1 \tag{6}$$

In this way, the time axis of the output is calibrated in frequency. The postmultiply is needed to obtain the proper phase of the DFT coefficients and can be omitted when phase is not required.

Several undesirable features of this implementation become apparent from the above description. The output must be blanked during the loading of the chirp into the filter, and the input must be set to zero during the calculation of the coefficients. Also undesirable is the inefficient use of the CCDs since only half of the CCD filter has useful information at any point in time.

For DFT applications, such as video bandwidth reduction,[18] in which the transform is to be inverted to regain the original signal, the CZT is performed in the way described above. However, when the spectral density is required, the CZT can be simplified greatly. Using the substitution of equation (4) in equation (3) gives

$$\left|F_k\right|^2 = \left| \sum_{n=0}^{N-1} f_n w_n e^{-i\pi n^2/N} \cdot e^{i\pi (k-n)^2/N} \right|^2 \tag{7}$$

In this case, simplification of the CZT algorithm results from two observations: (1) The postmultiply operation can be eliminated and (2) The sliding CZT can be used.

The sliding DFT is defined in this paper to be

$$F_k^s = \sum_{n=k}^{k+N-1} f_n e^{-i2\pi nk/N} \tag{8}$$

and it gives a windowed power density spectrum

$$\left|F_k^s\right|^2 = \left|\sum_{n=0}^{N-1} f_{n+k} w_n e^{-i2\pi nk/N}\right|^2 \quad (9)$$

$$= \left|\sum_{n=0}^{N-1} f_{n+k} w_n e^{-i\pi n^2/N} \cdot e^{i\pi(k-n)^2/N}\right|^2 \quad (10)$$

Comparison of equations (9) and (10) with equations (3) and (7) indicates that the sliding CZT differs from the conventional CZT in that the sliding CZT indexes the data each time a spectral component is calculated. For a periodic waveform, indexing results in a phase factor which does not affect the result, and for a stationary random signal, the time record is different for each spectral component but stationarity insures that the result is unaffected. For these two classes of signal the sliding CZT gives the same result as the conventional CZT.

Figure 4 gives a pictorial comparison between the conventional CZT and the sliding CZT for the simple case of a 3-point transform. With the conventional CZT, all three Fourier coefficients F_0, F_1, F_2 are calculated using the first three time samples f_1, f_2, f_3. These coefficients are being calculated by the filter during the next three clock periods, so that time samples f_4 - f_6 must be blanked. Then the cycle repeats as shown in Figure 4a. Using the sliding CZT, F_0^s is calculated on the sample record f_1, f_2, f_3 as before, but F_1^s is calculated on the sample record f_2, f_3, f_4; F_2^s on the record f_3, f_4, f_5, and the next F_0^s computation is made on the sample record f_4, f_5, f_6. The sample record is continually updated by replacing the oldest sample with a new one. The above description shows that N Fourier coefficients are obtained for N time samples (100% duty cycle).

The advantages of the sliding CZT are (1) For an N-point transform, N-stage filters are required which chirp through a bandwidth f_c ($-f_c/2$ to $+f_c/2$ for example). (2) No blanking is required. The filters operate with 100% duty cycle; i.e., one spectral component out for each time sample in. (3) Windowing can be achieved by weighting the chirp impulse response of the filter with the desired window function. (4) The degradation due to imperfect charge transfer efficiency is less for the sliding CZT than for the conventional CZT.

The block diagram for obtaining the spectral density using the sliding CZT is shown in Figure 5. The rectangles represent CCD filters having impulse responses $w_n \cos \pi n^2/N$ and $w_n \sin \pi n^2/N$, $-N/2 < n < N/2-1$. This system has been implemented using 500-stage CCD filters. The window function is coded into the metal photomask and systems have been demonstrated both without windowing ($w_n = 1$) and with Hamming windowing.[5] Spectra obtained using Hamming windowing are shown in Figure 6.

CCD PRIME TRANSFORM

Another algorithm exists for computing the DFT which is also suitable to CCD implementation in the analog domain because the bulk of the computation is performed in a transversal filter.[16,17] The prime transform algorithm is implemented in 3 steps as indicated in Figure 7; (1) permutation of the input data, (2) Transversal filtering and (3) permutation of the output Fourier coefficients. (for details see Reference 17) The advantages of the prime transform over the CZT are (1) the multipliers are replaced by permuting memories. (This may or may not be an advantage depending upon the speed and dynamic range required) and (2) For a real input, only two filters are required instead of the four shown in Figure 5. The disadvantages are (1) the zero order Fourier coefficient (dc term) must be computed separately (2) Imperfect charge transfer efficiency does not result in a simple degradation in resolution as it does in the CZT and (3) The sliding DFT cannot be implemented with the prime transform.

The CCD prime transform has not yet been tested but preliminary estimates suggest that it may be important for applications in which (1) the phase of the DFT is required thus ruling out the sliding CZT and (2) high speed and high dynamic range make on-chip multipliers difficult to implement.

IV. PERFORMANCE COMPARISONS

In this section some important comparisons are made between the CCD CZT and the digital FFT. Perhaps the most important point of comparison is accuracy. CCD's,

being analog, limit the accuracy of the CCD CZT. The major CCD limitations are (1) Charge transfer efficiency (CTE) (2) thermal noise (3) accuracy of the filter weighting coefficients (4) accuracy of the pre and post multipliers and (5) linearity of the CCD filters. With proper operation of the CCD filters it is expected that CCD operation can be made sufficiently linear that errors due to nonlinearities are not important. Each of the first four limitations is discussed in this section in the context of digital FFT comparison.

CTE affects the resolution of the DFT and is discussed separately. Thermal noise, weighting coefficient accuracy and multiplier accuracy are best discussed on terms of rms error in the transform. These sources of error are evaluated and related to the number of bits required to achieve equivalent error in an FFT. Finally, a state-of-the-art custom I^2L FFT is discussed and compared with the CCD CZT.

CTE

The effect of imperfect CTE is somewhat different for the conventional CZT than for the sliding CZT. In this section the sliding transform will be discussed.

The CZT is of course a sampled-data system, and the DFT is only defined for integral values of k. It is useful, however, to treat k as a continuously varying envelope which determines the spectral value at each integral k. Assuming the input is a complex sinusoid at frequency f, then equation (3) gives

$$\left|F_k\right|^2 = \left|\sum_{n=0}^{N-1} w_n e^{-i2\pi n\left(k - \frac{Nf}{f_c}\right)/N}\right|^2 \qquad (11)$$

We can treat F as a function of continuously varying k by writing

$$\left|F(k)\right|^2 = G\left(k - \frac{Nf}{f_c}\right) \qquad (12)$$

where the envelope function G(k) is the transform of the window function

$$G(k) = \left|\sum_{n=0}^{N-1} w_n e^{-i2\pi nk/N}\right|^2 \qquad (13)$$

The frequency resolution, sidelobe level etc. are all determined by G(k), and the effect of imperfect CTE is to broaden and shift the peak of G(k).

Equation (11) can be rewritten as

$$\left|F_k\right|^2 = \left|\sum_{n=0}^{N-1} e^{-i\pi(n+k-N\ f/f_c)^2/N}\ h_n\right|^2 \qquad (14)$$

where h_n is the ideal impulse response of a windowed chirp filter

$$h_n = w_n e^{i\pi n^2/N} \qquad n=0,\ N-1 \qquad (15)$$

Imperfect CTE modifies the weighting coefficients to h_n' and changes the envelope $G'(k)$ to

$$G'(k) = \left|\sum_{n=0}^{N-1} e^{-i\pi(n-k)^2/N}\ h_n'\right|^2 \qquad (16)$$

Physically G(k) represents the correlation of a chirp waveform in a windowed chirp filter and equation (16) shows how the correlation response degrades as the filter decorrelates due to imperfect CTE. The decorrelating effect can be crudely estimated by scaling the clock frequency down by a factor on the order of $1 - \varepsilon$, where ε is the fractional loss per stage.[11] This has the effect of decreasing the df/dt of the chirp filters by a similar factor with the result that the correlation peak broadens due to mismatch and shifts by an amount $\Delta t \sim N\varepsilon/2f_c$. This approximate behavior is confirmed by the calculations of Figure 8 which show the response of the 500-point sliding CZT with Hamming windowing to an input sinusoid having frequency $f = 3.3\ f_c/N$.

Conclusions regarding the effect of imperfect CTE on the sliding CZT are summarized below. (1) The resolution degradation is on the order of $N\varepsilon$ times the ideal resolution f_c/N. For $N\varepsilon \sim .1$, the degradation is negligible. (2) The degradation is the same for all frequencies whereas in the conventional CZT, the degradation is three times worse for the high frequencies than for the low frequencies, (3) The degradation can be eliminated by modifying the filter coefficients to compensate for imperfect CTE or by modifying the premultiply chirp.

ERROR ANALYSIS

The accuracy which can be achieved using the CCD CZT is perhaps the most important performance criterion. In this section, the error sources are identified and evaluated in terms of bits in an equivalent digital FFT.

FFT Accurancy. Finite word length effects in a digital FFT fall into three categories.[8,19,20] (1) Quantization of the data at the input A/D converter. (It is assumed that no external gain control is used with either the FFT or the CCD CZT). (2) Errors due to the finite word lengths used to represent the twiddle factors.[19] (3) Truncation and roundoff effects generated within the butterflies.[20] In treating truncation effects a block floating point truncation algorithm is assumed in which all words are shifted right each time overflow occurs in any butterfly.

If the A/D converter has an accuracy of b_1 bits plus a sign bit, the quantization step size is 2^{-b_1} normalized to unity, and an rms error can be defined by

$$\Delta_Q = \left[\frac{1}{N}\sum_{n=0}^{N-1}\left(f_n - f_n^Q\right)^2\right]^{\frac{1}{2}} \qquad (17)$$

$$= 2^{-b_1} / \sqrt{12} \qquad (18)$$

This noise does not scale with signal size. It represents a noise level below which signals cannot be processed. It dominates at low signal levels but other errors which scale with signal size dominate FFT error at large signal size.

If the twiddle factors are quantized to b_2 bits plus sign, the resulting rms error is given by[19]

$$\Delta_T = \frac{\log_2 N}{6}\, 2^{-b_2}\, \sigma_F \qquad (19)$$

where σ_F is the rms level of the output signal and is related to the rms input signal σ_f through $\sigma_F = \sqrt{N}\ \sigma_f$.

The most important source of error in a digital FFT is usually overflow and roundoff of data words during butterfly computation. If the data words are carried with b_3 bits plus sign, an upper bound on error in a block floating point machine can be determined assuming overflow occurs at every stage. The result is[20]

$$\Delta_B = .3\sqrt{8}\, N^{\frac{1}{2}}\, 2^{-b_3} \qquad (20)$$

If the twiddle factors are quantized to the same accuracy as the data words ($b_2 = b_3$) Δ_B dominates FFT error. Although equation (20) does not contain the input signal size explicitly. Δ_B does scale in a general way with signal because for smaller signals, overflow does not occur at every stage. The dependence of Δ_B on the length of the transform indicates that higher accuracy (large b_3) is required for longer transforms.

CCD CZT Accuracy. The sources of error in a CCD CZT are (1) thermal noise, (2) quantization of the pre and post multiply chirp waveforms, (3) weighting coefficient error in the CCD transversal filters, and (4) CTE. When the criterion of rms error to rms signal is applied, imperfect CTE generates large errors, because the errors add coherently. Because of this fact, however, CTE effects can be treated as a resolution degradation as discussed above and not as "random" error.

Thermal noise is analogous to input quantization in a digital FFT because it generates an error which is independent of signal size. Thermal noise in the CCD CZT is dominated by noise in the output amplifier of the filter.[5] Assuming the rms noise referred to the input is 60 dB below the maximum peak signal, the equivalent quantization accuracy is $b_1 = 8$ bits plus sign. If 80 dB can be achieved[5] this will correspond to $b_1 = 11\frac{1}{2}$ bits plus sign. At higher signal levels thermal noise, like input quantization noise in a digital FFT, is dominated by signal dependent errors.

In implementing the CCD CZT, the pre and post multiply chirp waveforms can be stored digitally in a ROM and multiplication can be performed in multiplying D/A converters.[21] If the waveforms are stored with an accuracy of b_4 bits plus sign, the errors are analogous to twiddle factor quantization in a digital FFT. The calculated rms output levels Δ_M for both the pre and post multipliers is

$$\Delta_M = \frac{2^{-b_4}}{\sqrt{12}}\ \sigma_F \qquad (21)$$

In Figure 9 the rms error to rms signal (Δ_M/σ_F) is plotted as b_4. The solid line is calculated using equation (21). The points are obtained from computer simulation of a 32-point CCD CZT. The input data were normally distributed random numbers. However, similar results are obtained using sine waves.

Weighting coefficient error arises from a number of sources, but let us assume as a model, that the placement of the gap in the split electrodes is quantized in steps of δ during photomask fabrication. δ is typically 10 μin and the channel width W is typically 5 mil giving $\delta/W = .002$ this is equivalent to quantizing the weighting coefficients to 8 bits plus sign and is again analogous to twiddle factor quantization. The error which results is given by

$$\Delta_W = \frac{1}{\sqrt{6}} \frac{\delta}{W} \sigma_F \qquad (22)$$

A plot of this expression together with computer simulated results are given in Figure 10.

Comparison. The major source of FFT error increases like $\sqrt{N}$ (equation 20) whereas the major sources of CCD CZT error are independent of transform length.

Figure 11 compares the digital FFT with the CCD CZT using as the criterion the ratio of rms error to rms signal for large signals. The results are plotted as a function of the transform length N. A word length of 13 bits plus sign was assumed for the data and twiddle factors and on this case Δ_B dominates FFT error. For the CCD CZT, the multiplying chirp waveforms are quantized to 7 bits plus sign and $\delta/W = .002$.

CUSTOM FFT

In evaluating the potential of the CCD CZT, it is important to compare it, not with currently existing digital implementations of the FFT, but with projected state-of-the-art implementations which are under development. A potential digital competitor for the analog CCD spectrum analyzer is a custom FFT,[2] and a low-power LSI FFT system using all I^2L technology is presented here for comparison.

A few introductory statements concerning the state of I^2L and the design philosophy of the custom FFT presented here are appropriate. I^2L is a very low-power, high density technology currently in early stages of product development. Current devices are running at speeds up to 2 MHz, but it is expected that speeds will improve significantly as the technology matures. The hypothetical FFT design presented here is custom in the sense that the architecture is tailored to perform the algorithm relatively efficiently and has matched the memory and computation speeds. None of the chips have actually been built, but are believed to be within the state-of-the-art. Flexibility normally expected in an FFT is provided, and with additional firmware, other vector oriented algorithms could be implemented. Therefore, this design can be considered as a general purpose digital signal processing module.

Table 1 lists the specifications of a hypothetical FFT processor.

Table 1. FFT Specifications

Algorithm	Inplace
Cycle Clock	2 MHz
Butterfly Time	4 μsec
Transform Speed*	N/2 log (N+1) x Butterfly Time
Transform Lengths	N=1,2,3,..,512 complex points
Arithmetic	16 bit block floating point with rounding
Coefficient Word Length	8 bits
Data Word Length	16 bits

*Include unscrambling.

The processor is designed from three basic I^2L chips: a single control chip, a 4 bit arithmetic unit slice, and a 1024 x 4 bit RAM slice. The control chip includes the coefficient memory, the FFT microporgram memory, and the control and address generation circuitry. The arithmetic slice is a complex arithmetic unit (CAU) tailored to perform a parallel FFT (radix-2) Butterfly operation. Although the processor can be configured in multiplies of these 4 bit slices, a 16 bit configuration, sketched

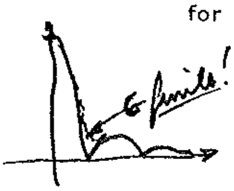

CCD CZT Performance Limits

Parameter	Function	Value
Transform length	ε bin size	103
time resn	leakage	1sec ← (maximum signal down by 6dB.)
speed	analog clock.	5MHz.
accuracy. reset	[illegible] quantizat 8 BITS	13-bits 5%

in Figure 12, has been chosen as a prototype model. Itemized power estimate of this processor with a 500 nanosecond cycle time is 300 mW dominated by the memory.

The I^2L hypothetical FFT processor described above has overwhelming advantages over the CCD CZT in (1) flexibility and (2) accuracy in a sense that additional slices can be added. However, when flexibility and high accuracy are not required the CCD CZT compares favorably in two important aspects. (1) Number of packages: The 512-point sliding CZT illustrated in Figure 5 can be implemented with 3 IC's; 2 CCD filter IC's and one ROM containing the premultiply chirp. The I^2L digital processor requires 9 IC's (see Figure 12) and in addition, requires A/D conversion. Even when state-of-the-art custom digital hardware is postulated, the CCD CZT maintains a clear cut advantage in package count and hence cost. (2) Speed: The I^2L FFT operating at it's maximum clock rate (2 MHz) generates spectral points at a 50 kHz rate. In general digital FFT hardware is limited to this kind of speed, and increased speed through parallel processing can be achieved only by a proportional increase in hardware. The CCD CZT, on the other hand operates in real time at speeds up to 5 MHz.

CCD's have also been proposed to perform the digital functions required to implement the FFT,[22,23] and it has been claimed that, compared to competing devices from other technologies, "charge-coupled devices appear to enjoy a ten to one advantage in device density and greater than a ten to one advantage is speed-power product".[23] Detailed comparisons with competing technologies need to be made to substantiate this claim.

V. APPLICATIONS OF THE CCD CZT

For a given spectral analysis application to be considered as a candidate for CCD CZT implementation it must satisfy two criteria: (1) It must be of modest performance which lies within the CCD performance limitations and (2) It must be required in sufficiently high volume that low cost is a dominant design specification. These two criteria rule out a large class of applications. However, there have been identified, several applications of great military importance which do satisfy both of the above criteria. These will be discussed in this section.

VIDEO BANDWIDTH REDUCTION

Transform encoding of video images for the purpose of bandwidth reduction is a potentially important application of the CCD CZT. A hybrid transform system has been developed[18] which performs a discrete cosine transform (DCT) in one dimension and differential pulse code modulation (DPCM) in the other dimension.

DFT and DCT on "typical" video images have resulted in variance compaction approaching that of optimum transforms,[18] and both the DFT and DCT can be cost effectively implemented with the CCD CZT. The CCD CZT becomes particularly attractive in remote sensing applications such as RPV's where small size, light weight, and low power are essential in addition to low cost.

SPEECH PROCESSING

Spectral analysis is one of the most important functions in speech processing,[24] and speech processing requirements in terms of sample rate (10 kHz), delay time (40 ms) and dynamic range (40 dB) are well within the CCD capabilities outlined above.

The simplest speech processing systems decompose speech into its spectral components as in the early channel vocoder systems. Channel vocoders perform well only at high bit rates[25] and therefore do not achieve optimal bandwidth reduction, but they are useful in word recognition systems.

There exist several algorithms which do achieve adequate bandwidth reduction and of these, one, is particularly well suited to CCD implementation. It is called homomorphic deconvolution[26] and operates upon the principle of the deconvolution of speech into pitch and to vocal tract resonances. In Figure 13 a block diagram of such a system is shown.[24] Since only the magnitude of transform 1 is required, the postmultiply can be eliminated, and in addition, the postmultiply of the inverse transform 2 cancels the premultiply of transform 3. Therefore the only chirp multiplications remaining are the premultiplies of transforms 1 and 2 which can be implemented at the input to the CCD.[27] After transform 2, the pitch of the voiced speech is detected and then windowed out so that only the smoothed speech spectrum remains at the output. This spectra can be used to extract

formant data and if this information is efficiently encoded data rates as low as 1000 bits/s are realizable.[24] Homomorphic deconvolution is costly to implement digitally in real time because of the three sequential transforms which are required. However, the CCD CZT holds the promise of truly low cost implementations of this type of processing.

DOPPLER PROCESSING IN MTI RADAR

MTI (moving target indicator) radar operates upon the principle of detecting moving targets of small cross section in the presence of stationary background having much larger cross section. The doppler shift of the radar return is determined, and from this, the target velocity parallel to the radar line of sight, can be determined.

Radar returns are quasi-periodic, and the sliding CZT can be used. Typical transform lengths are 10 to 100 and typical pulse repetition frequency (PRF) is 1 kHz to 100 kHz. A doppler processor may be required to process thousands of DFT's on parallel, (one for each range gate) so reducing the cost of the DFT has a large cost impact on the overall system.

A doppler processor IC has been developed [28,29] which performs ten 17-point CCD CZT's of the type shown in Figure 5. The IC contains all the integrated amplifiers and squaring circuitry required to obtain the power density spectrum in each range bin. A doppler processor for thousands of range bins can be implemented by cascading 10-bin IC's at a projected cost of approximately one-third that of an all digital processor designed using state-of-the-art digital hardware.[28]

OTHER APPLICATIONS

Other potential applications of the CCD CZT include processing for FLIR images, sonobuoy signal processing, and remote surveillance.

The CCD CZT is not expected to make the digital FFT obsolete in military sistems. However, for those spectral analysis applications which fulfill the twin requirements of modest performance and high volume, tremendous cost advantages can be gained using the CCD CZT. More applications will certainly emerge, but in the meantime, the potential cost impact in the application areas already identified guarantees the importance of the CCD CZT in military electronic signal processing systems of the future.

ACKNOWLEDGEMENT

Development of the CCD CZT at Texas Instruments has been sponsored by the Army Electronics Command (Robert H. Sproat, contract monitor) and by the Defense Advanced Research Projects Agency/Naval Undersea Center (Dr. Robert W. Means, contract monitor).

REFERENCES

1. H. J. Whitehouse, J. M. Speiser and R. W. Means, "High Speed Serial Access Linear Transform Implementations," presented at the All Applications Digital Computer Symposium, Orlando, Florida, 23-25 January 1973. NUC TN 1026.

2. L. R. Rabiner, R. W. Schafer, and C. M. Rader, "The Chirp Z-Transform Algorithm," IEEE Trans. on Audio and Electroacoustics, AU-17, pp. 86-92, June 1969.

3. R. W. Means, D. D. Buss, and H. J. Whitehouse, "Real Time Discrete Fourier Transforms Using Charge Transfer Devices," Proc. CCD Applications Conference, San Diego, pp. 127-139, September 1973.

4. R. W. Brodersen, H. S. Fu, R. C. Frye, and D. D. Buss, "A 500-point Fourier Transform Using Charge-Coupled Devices," 1975 IEEE International Solid-State Circuits Conference, Digest of Technical Papers, Phila, February 1975, pp 144-145.

5. R. W. Brodersen, C. R. Hewes and D. D. Buss, "Spectral Filtering and Fourier Analysis Using CCD's," IEEE Advanced Solid-State Components for Signal Processing, IEEE International Symposium on Circuits and Systems, Newton, Mass., pp 43-68, April 1975.

6. G. D. Bergland, "A Guided Tour of the Fast Fourier Transform," IEEE Spectrum, Vol. 6, pp. 41-52, July 1969.

7. W. M. Gentleman, and G. Sande, "Fast Fourier Transform - for Fun and Profit," 1966 Fall Joint Computer Conf. AFIPS Proc., Vol. 29, Washington, D.C.:

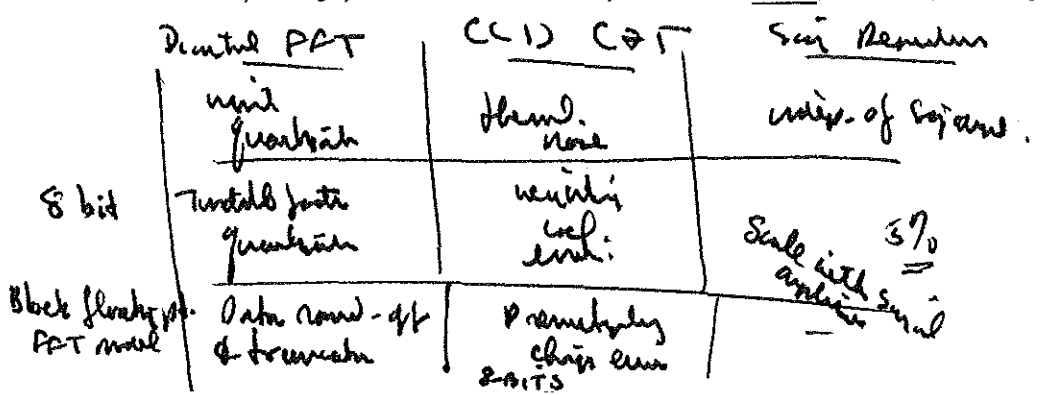

Spartan, 1966, pp. 563-578.

8. L. R. Rabiner and B. Gold, Theory and Application of Digital Signal Processing, Prentice-Hall, 1975, Ch.6.

9. P. R. Hariharan, and R. J. Scott,"Effects of Ideal Clipping on Signal-to-Noise Ratios - A Comparison with Linear Systems," 84th Meeting of Acoustical Society of Am, 30 Nov. 1972, Paper Y.6, The Magnavox Co, Fort Wayne, Indiana, 46804.

10. D. D. Buss, D. R. Collins, W. H. Bailey, and C. R. Reeves, "Transversal Filtering Using Charge Transfer Devices," IEEE J. Solid-State Circuits, SC-8, pp 134-146, April 1973.

11. D. D. Buss and W. H. Bailey, "Application of Charge Transfer Devices to Communication," Proc. CCD Applications Conference, San Diego, September 1973, pp 83-93.

12. R. D. Baertsch, W. E. Engeler, H. S. Goldberg, C. M. Puckette, and J. J. Tiemann, "Two Classes of Charge Transfer Devices for Signal Processing," Proc. International Conf. Technology and Applications of CCDs, Edinburgh, Sept. 1974, pp 229-236.

13. A. Ibrahim and L. Sellars, "CCDs for Transversal Filter Applications," IEEE International Electron Devices Meeting, Technical Digest, Washington, Dec. 1974, pp 240-243.

14. J. A. Sekula, P. R. Prince and C. S. Wang, "Non-Recursive Matched Filters Using Charge-Coupled Devices," IEEE International Electron Devices Meeting, Technical Digest, Washington, Dec. 1974, pp 244-247.

15. M. F. Tompsett, A. M. Mohsen, D. A. Sealer, and C. H. Sequin, "Design and Characterization of CCD's for Analog Signal Processing," IEEE Advanced Solid-State Components for Signal Processing, IEEE International Symposium on Circuits and Systems, Newton, Mass., pp 83-89, April 1975.

16. H. J. Whitehouse, R. W. Means, and J. M. Speiser, "Signal Processing Architectures Using Transversal Filter Technology," IEEE Advanced Solid-State Components for Signal Processing, IEEE International Symposium on Circuits and Systems, Newton, Mass., April 1975, pp 5-29.

17. C. M. Rader, "Discrete Fourier Transforms When the Number of Data Samples is Prime," Proc. IEEE 56, pp 1107-1108, June 1968.

18. R. W. Means, H. J. Whitehouse and J. M. Speiser, "Television Encoding Using a Hybrid Discrete Cosine Transform and a Differential Pulse Code Modulator in Real Time," 1974 National Telecommunications Conference Record, SAn Deigo, Dec. 1974, pp 69-74.

19. C. J. Weinstein, "Roundoff Noise in Floating Point Fast Fourier Transform Computation," IEEE Trans. Audio Electroacoustic, AU-17, pp 209-215, September 1969.

20. P. D. Welch, "A Fixed-Point Fast Fourier Transform Error Analysis," IEEE Trans. Audio Electroacoustic, AU-17 pp 151-157, June 1969.

21. R. W. Means, NUC Private Communications.

22. C. S. Miller and T. A. Zimmerman, "The Application of Charge-Coupled Devices to Digital Signal Processing," International Conference on Communications Conf. Record Vol.I, San Francisco, June 1975, pp 2/20-2/24.

23. T. A. Zimmerman, "The Digital Approach to Charge-Coupled Device Signal Processing," IEEE Advanced Solid-State Components for Signal Processing, IEEE International Symposium on Circuits and Systems, Newton, Mass., April 1975, pp 69-82.

24. R. W. Schafer and L. R. Rabiner, "Digital Representations of Speech Signals," Proc. of the IEEE 63, pp 662-677, April 1975.

25. R. W. Schafer and L. R. Rabiner, "Design of Digital Filter Banks for Speech Analysis," BSTJ, 50, pp 3097-3115, Dec. 1971.

26. A. V. Oppenheim and R. W. Schafer, "Homomorphic Analysis of Speech," IEEE Trans. Audio. Electroacoustic, Vol AU-16, pp 221-226, June 1968.

27. D. A. Hodges, U.C. Berkeley, Private Communication.

28. D. D. Buss, W. H. Bailey, M. M. Whatley and R. W. Brodersen, "Application of Charge-Coupled Devices to Radar Signal Processing," 74 NEREM Record, Boston, Nev. 1974, pp 83-98.

29. W. H. Bailey, D. D. Buss, L. R. Hite and M.M. Whatley, "Radar Video Processing Using the CCD Chirp z-Transform," This Conference.

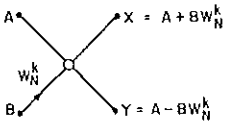

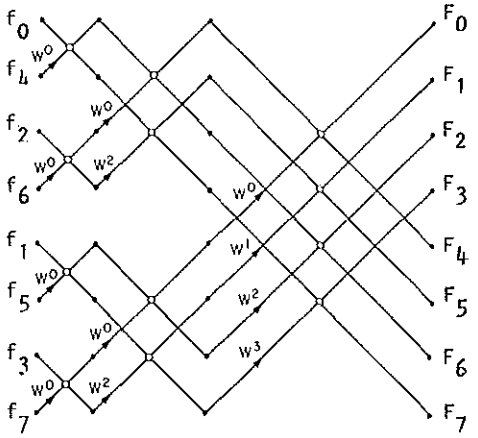

Fig. 1 a) Schematic of the butterfly. (see Eq. (2)) b) Schematic of an 8-point, radix 2, decimation in time FFT (Ref. 8)

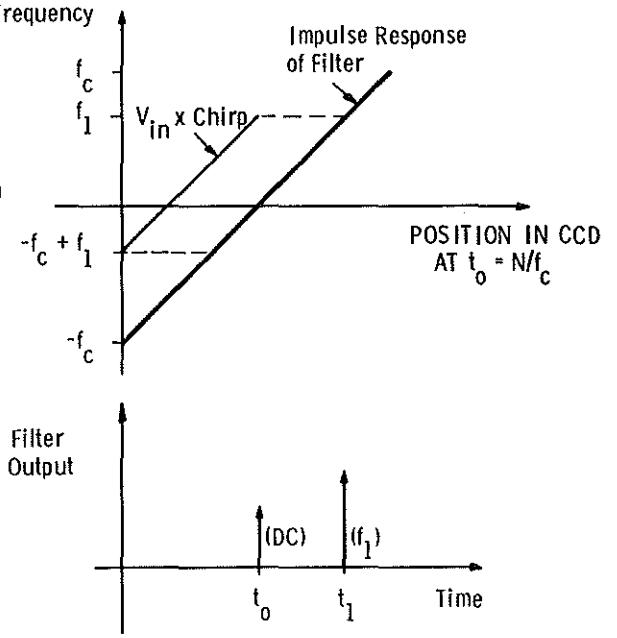

Fig. 3 Interpretation of the CZT in terms of chirp input waveforms in chirp filters.

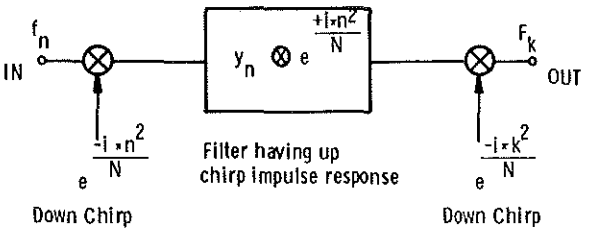

Fig. 2 Schematic of the CZT algorithm.

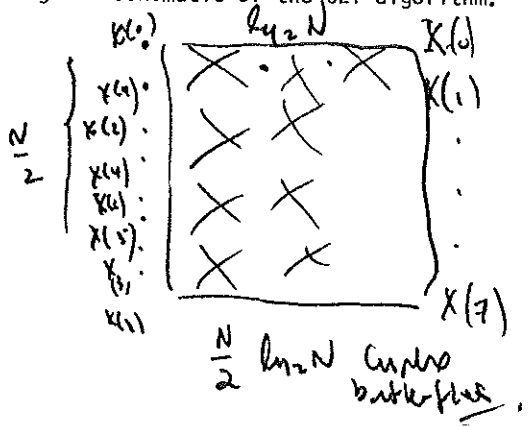

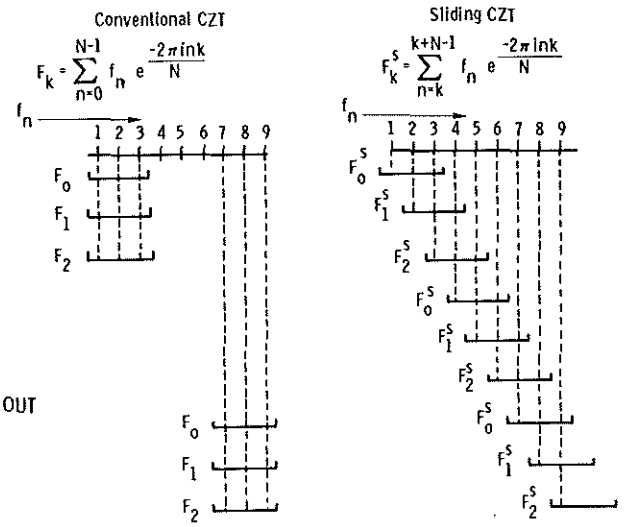

Fig. 4 Comparison between the conventional CZT and the sliding CZT for the case of a 3-point transform.

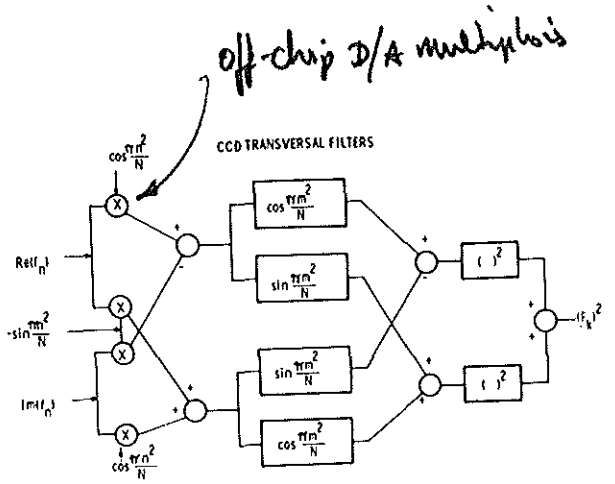

Fig. 5 An implementation of the CZT algorithm using real components. The power density spectrum $|F_k|^2$ is computed for an input which has both real (in-phase) and imaginary (quadrature) components.

Developed for NASA/GSFC

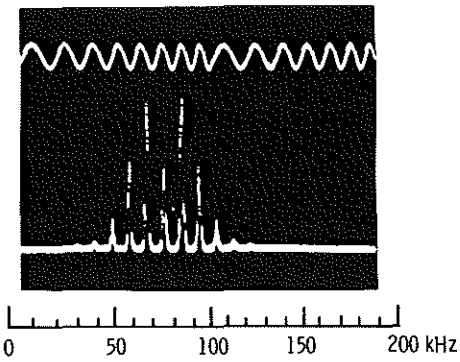

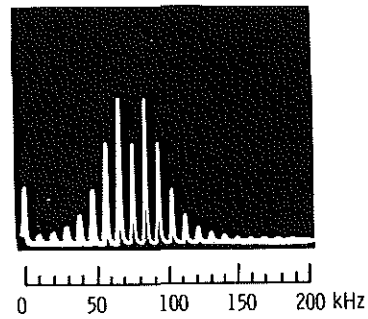

Fig. 6 A comparison of the 500-point sliding CZT power density spectrum (upper photograph) with the output of a conventional spectrum analyzer (lower photograph which shows the square root of the power density spectrum).

The input signal shown at the top of the upper photograph chirps from 50 kHz to 100 kHz with a repetition period of T_d = 110 μsec. This results in a line spectrum having period T_d^{-1} = 9 kHz.

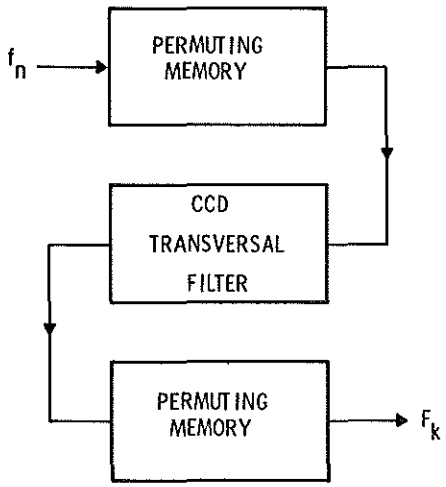

Fig. 7 Block diagram of the prime transform implemented with CCDs.

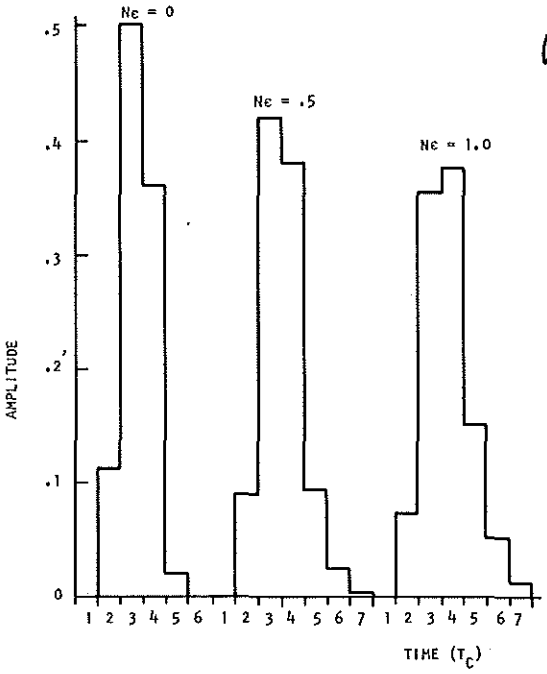

Fig. 8 The calculated response of the 500-point sliding CZT with Hamming weighting to a complex input sinusoid of frequency $f_{in} = \frac{3.3}{N} f_c$. The response is calculated for different values of CTE.

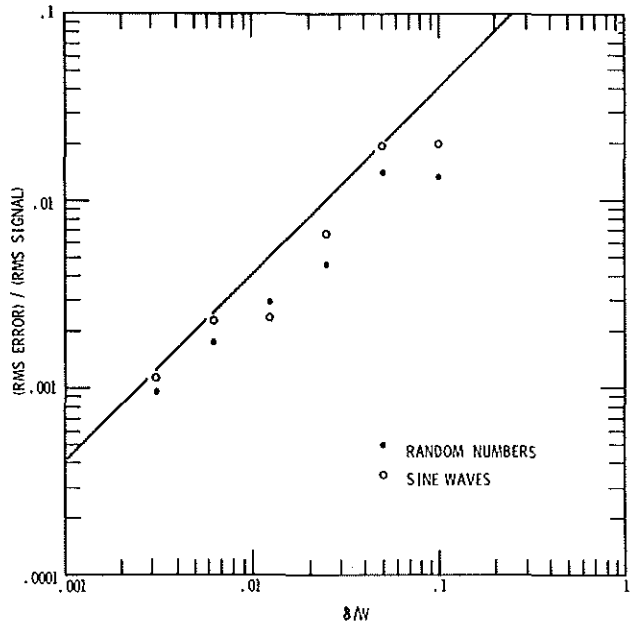

Fig. 9 Error to signal ratio Δ_M computed as a function of the number of bits b_4 used to quantize the premultiply and postmultiply chirp waveforms. The line represents Eq. (21). The points represent computer simulation in which just the premultiply or postmultiply is quantized.

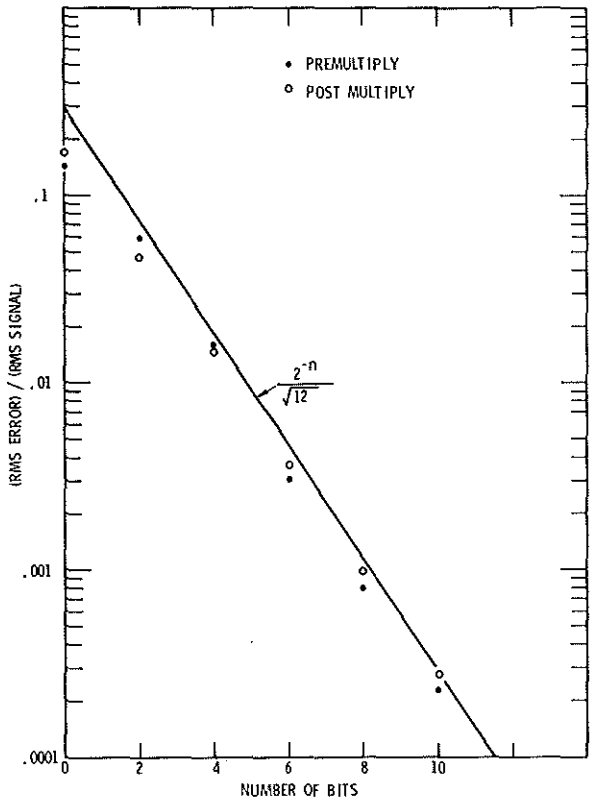

Fig. 10 Error to signal ratio Δ_W computed as a function of weighting coefficient error δ/W. The solid line represents Eq. (22). The points represent computer simulation for random numbers and sine waves.

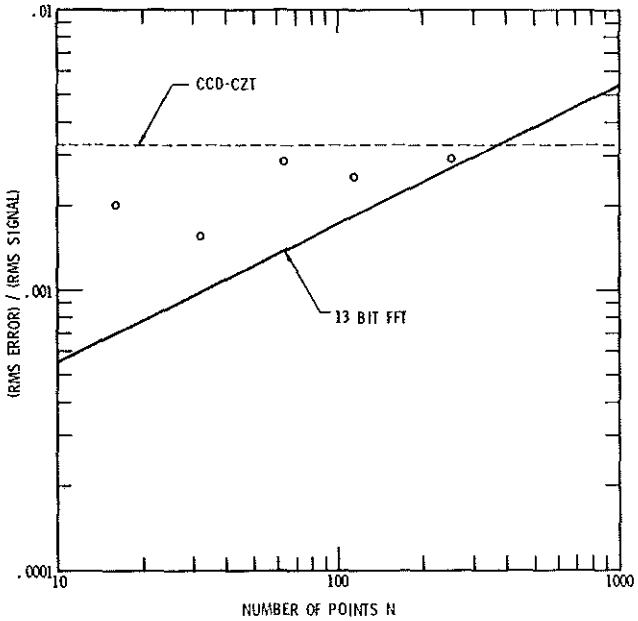

Fig. 11 Error comparison between a CCD CZT and a digital FFT implemented using 13 bits plus sign. The CCD CZT is limited by the quantization of multiply chirps to 7 bits plus sign. The points represent computer simulation for the CCD CZT.

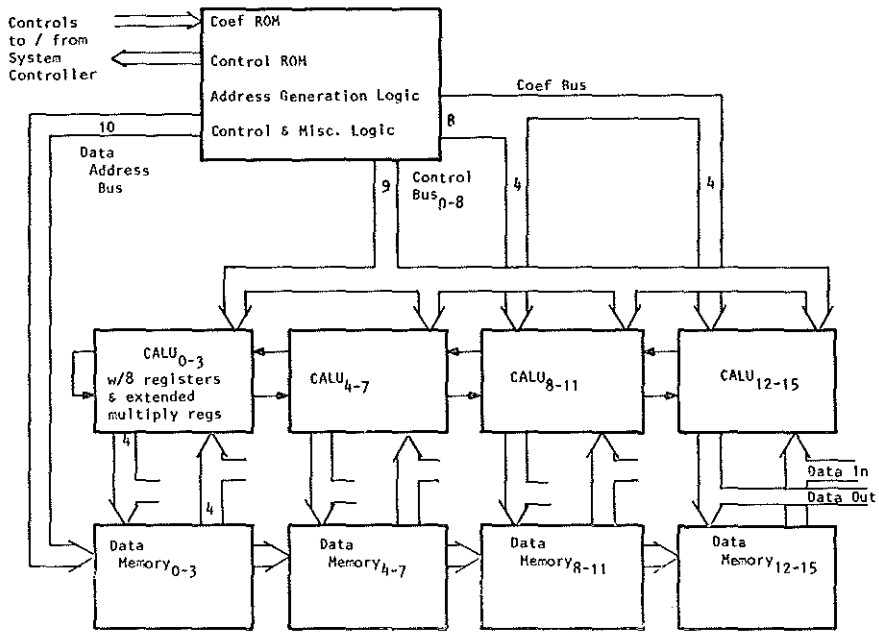

Fig. 12 A custom 16 bit I^2L FFT requiring 9 IC's.

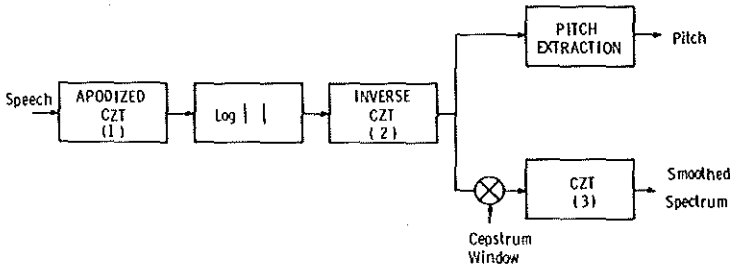

Fig. 13 Block diagram of a system to perform homomorphic deconvolution of speech for bandwidth reduction (Ref. 24). This is one type of speech processing which is particularly amenable to implementation with CCDs.

Applications:
Video BW reduction (RADV)
Speech processing
Doppler Processing in Radar (MTE)
Sonobuoy Signal Processing
Image Processing (ELER)
Remote Surveillance.

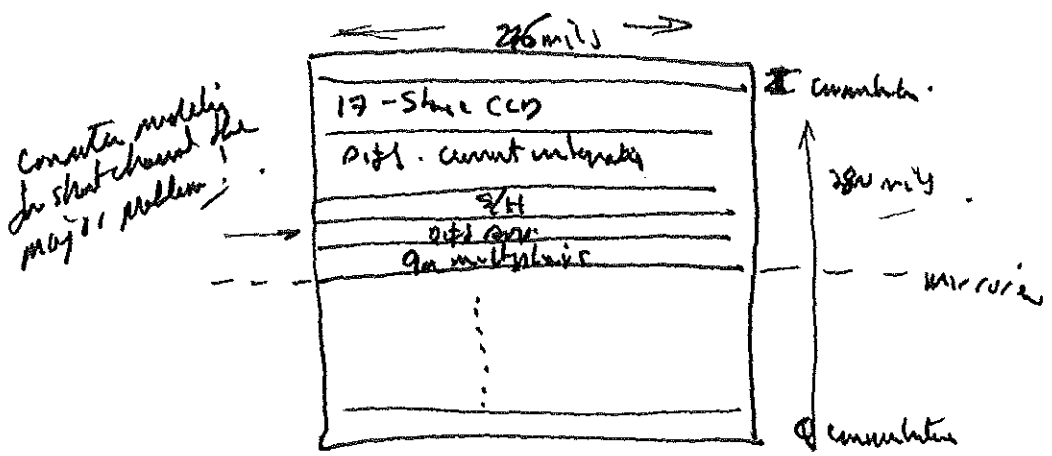
17 - Stage CCD
S/H